

CLASTER: Clustering with Reinforcement Learning for Zero-Shot Action Recognition

Shreyank N Gowda¹

s.narayana-gowda@sms.ed.ac.uk

Laura Sevilla-Lara¹

l.sevilla@ed.ac.uk

Frank Keller¹

frank.keller@ed.ac.uk

Marcus Rohrbach²

mrf@fb.com

¹University of Edinburgh

²Facebook AI Research

Abstract

Zero-shot action recognition is the task of recognizing action classes without visual examples, only with a semantic embedding which relates unseen to seen classes. The problem can be seen as learning a function which generalizes well to instances of unseen classes without losing discrimination between classes. Neural networks can model the complex boundaries between visual classes, which explains their success as supervised models. However, in zero-shot learning, these highly specialized class boundaries may not transfer well from seen to unseen classes. In this paper we propose a clustering-based model, which considers all training samples at once, instead of optimizing for each instance individually. We optimize the clustering using Reinforcement Learning which we show is critical for our approach to work. We call the proposed method CLASTER and observe that it consistently improves over the state-of-the-art in all standard datasets, UCF101, HMDB51 and Olympic Sports; both in the standard zero-shot evaluation and the generalized zero-shot learning.

1. Introduction

Research on action recognition in videos has made rapid progress in the last years, with models becoming more accurate and ceiling performance being reached on some datasets. However, much of this progress has hinged on large scale training sets. In practice though, it is not practical that each time we want a network to recognize an additional class, we collect thousands of video samples. This idea has led to research in the zero-shot learning (ZSL) domain, where training occurs in a set of seen classes, and testing occurs in a set of unseen classes. In particular, in the case of video ZSL, class labels are typically “enriched” with semantic embeddings (which are sometimes manually annotated and some other times inferred automatically)

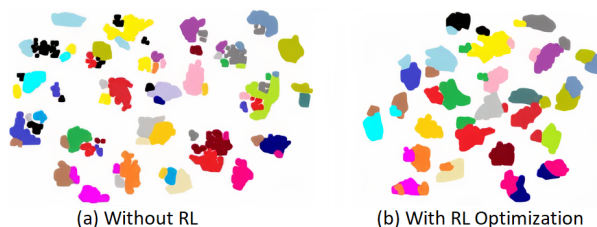


Figure 1. CLASTER improves the representation and clustering in unseen classes. The figure shows t-SNE [21] of video instances, where each color corresponds to a unique unseen class label. Our reinforcement learning (RL) optimization improves the representation by making it more compact: in (b) instances of the same class, i.e. same color, are together and there are less outliers for each class compared to (a).

that help transferring the knowledge from the seen training classes, to the new unseen classes. In the typical prediction pipeline, at test time a seen class is predicted, and its semantic embedding is used to search for a nearest neighbor in the space of the semantic embeddings of unseen classes. The predicted class will be the class corresponding to the nearest neighbor. While ZSL is potentially a very useful technology, it also presents large challenges. In particular, it requires learning a transfer function that discriminates unseen classes. This transfer function is defined using the semantic embeddings of each class, and therefore it is defined at the class level. This presents a challenge especially in the case of large intra-class variability, and at boundaries of similar classes, like “horse racing” and “horseback riding”.

The power of neural networks is that they are very good at learning complex discrimination functions of classes of with many modes, i.e. instances of the same class can be very different and still be projected by the neural network to the same category. While this works well in supervised training, this can be a problem in zero-shot recognition, where the highly specialized discrimination function might not transfer well to instances of unseen categories. In this

work, we turn to clustering which considers all training instances at once rather than optimizing for classifying single instances. The intuition here is that all instances of a class, while different from each other, belong to the same cluster, simplifying the classification problem. At the same time, classes that are too similar and difficult to discriminate belong to different clusters. Specifically, we use Reinforcement Learning (RL) to optimize the clustering, so that the signal of the classification can be used to learn the clusters. To keep the strong discrimination power we combine a cluster centroid representation with an instance level feature representation for the final classification. As we can see in Figure 1 our approach leads to less noisy and compact representations for unseen classes. We call our proposed method CLUSTER, for *CLustering for Action recognition in zero-ShoT lEaRning*, and show that it significantly outperforms all existing methods across all standard zero-shot action recognition datasets, and all zero-shot tasks.

Another challenge of ZSL is finding the mapping from seen classes to unseen classes without any visual cues. It is common to use semantic embeddings obtained with embedding models such as word2vec [24] on the class labels. In image datasets word embeddings work well, as they can capture hierarchical relationships among labels which are represented as nouns. Action classes on the other hand are typically represented by verbs, and often have more than one word per label. Previous work [10, 22, 25] averages the embeddings of each word in a multi-word label, to obtain a single semantic embedding for a class. However, as we show in this paper, this does not always capture the inter-dependency among action classes. Hence, we propose the use of sentence2vec [28], a model that is designed for sentence embeddings rather than word embeddings. As action classes are tagged with multi-word labels, using sentence2vec results in more accurate semantic class representations. We explain this in section 3.8 and visualize the differences in embeddings. Including this also into CLUSTER, we obtain a total of up to 11% improvement over previous state-of-the-art methods.

Contributions: Our main contribution is CLUSTER, a novel model for zero-shot learning which learns a clustering-based representation optimized with reinforcement learning (RL). Clustering with RL has not previously been explored for this task, and we show in our ablations that the RL optimization is the critical aspect of our approach. In our experimental evaluation we find that CLUSTER consistently outperforms prior work on three challenging zero-shot action recognition benchmarks, Olympics, HMDB51, and UCF101, both, in zero-shot learning and in the more challenging generalized zero-shot learning (GZSL) task. While we observe consistent improvements independent of the semantic embeddings employed, we show the importance of using sentence-level em-

beddings such as sentence2vec for zero-shot action recognition, as actions are frequently described with multiple words. This improves performance of both our model and prior work. Our improvements over previously reported results are substantial, e.g. we achieve 50.2% accuracy for ZSL on UCF101 (vs. prior best 43.0% [10]) and 47.4% accuracy on GZSL on HMDB51 (vs. prior best 36.1% [22]).

2. Related Work

Traditional Fully Supervised Action Recognition. The seminal work of Simonyan and Zisserman [35] introduced the now standard two-stream framework, which combines spatial (i.e. RGB) and temporal (i.e. optical flow) information. Also widely used are the spatio-temporal CNNs in C3D [37], P3D Resnet [30] and I3D [3], which has become one of the most commonly used off-the-shelf methods, and is a backbone for many applications, including this work. More recently, action recognition methods have become more sophisticated, using attention [38, 11] and leveraging the multi-modal nature of videos [2]. The work most related to ours is Ji et al. [13], who proposed the use of knowledge maps for coarse-to-fine action recognition. We build on this idea and use clusters as coarse representatives for classes, later refined to obtain a fine-grained classification result.

Zero-shot Learning. Early approaches followed the idea of learning semantic classifiers for seen classes and then classifying the visual patterns by predicting semantic descriptions and comparing them with descriptions of unseen classes. Lampert et al. [17] propose direct attribute prediction, which infers the posterior of each semantic description and calculate class posteriors, and indirect attribute prediction [17], which computes semantic posteriors from the class posterior of seen categories. Follow up work showed how to replace the manual attributes with automatically mined semantic relatedness [32]. The SJE model [1] uses multiple compatibility functions to construct a joint embedding space. ESZSL [33] uses a Frobenius norm regularizer to learn an embedding space. In videos, there are additional challenges: action labels need more complex representations than objects and hence give rise to more complexity in recognition and transfer.

ZSL for Action Recognition. Early work [31] was restricted to cooking activities, using script data to transfer to unseen classes. Gan et al. [8] consider each action class as a domain, and address semantic representation identification as a multi-source domain generalization problem. Manually specified semantic representations are simple and effective [44] but labor-intensive to annotate. To overcome this, the use of label embeddings has proven popular, as only category names are needed. Xu et al. [41, 40] use label embeddings to build a common embedding space between class labels and video features. The use of error-correcting codes

was proposed by [29]. Some approaches use pairwise relationships between classes [6] or inter-class relationships [7]. An out-of-distribution detector has been used along with GANs [22] to aid GZSL. Graph Neural networks have also been used for ZSL [10].

Reinforcement Learning for Zero-Shot Learning. RL for ZSL is a research topic that has only recently received attention. To the best of our knowledge, there is no other work using RL for zero-shot action recognition. RL for ZSL in images was introduced by Liu et al. [19] by using a combination of ontology and RL. They use RL to adaptively determine the discriminative degree of hierarchical classification rules. For zero-shot text classification, Ye et al. [42] propose a self-training method to efficiently leverage unlabeled data. They use the RL framework to learn a data selection strategy automatically and provide a more reliable selection. RL has been used in the zero-shot setting for problems such as task generalization [27], active learning [4], and video object segmentation [12].

3. CLUSTER: Clustering with RL for Zero-Shot Action Recognition

In this section we describe our proposed method, CLUSTER, which leverages clustering of visual and semantic features for video action recognition and optimizes the clustering with RL. Figure 2 shows an overview of the method.

3.1. Problem Definition

Let S be the training set of seen classes. S is composed of the tuples $(x, y, a(y))$, where $x \in X$ represents the spatio-temporal features of a video (in our experiments, a pre-trained I3D [3] network, using both RGB and optical flow, concatenated) in the space of possible video representation X , y represents the class label in the set of Y_s seen class labels, and $a(y)$ denotes the category-specific semantic representation of class y . These semantic representations are manually annotated in some datasets and computed using a word2vec representation in other datasets.

Let U be the set composed of pairs $(u, a(u))$, where u is a class in the set of unseen classes Y_u and $a(u)$ are the corresponding semantic representations. The seen classes Y_s and the unseen classes Y_u do not overlap.

The zero-shot learning (ZSL) task is to train a classifier that takes as input a visual video representation and outputs a class label of the unseen classes, as $f_{ZSL} : X \rightarrow Y_U$. In generalized zero-shot learning (GZSL), the task is to train a classifier that takes as input a visual video representation and outputs a class label of the union of the seen and unseen classes, as $f_{GZSL} : X \rightarrow Y_S \cup Y_U$. In the GZSL task, we use a bias detector following Gao et al. [9], to decide if the video belongs to a seen class or an unseen class.

3.2. Cluster Initialization

We cluster all instances in the training set S . We initialize the clusters with the k-means [5] algorithm and then optimize the centroids with reinforcement learning. We now describe the initial clustering process, and the optimization in Section 3.5.

We first need to combine the visual features x_i and the semantic representation $a(y_i)$ of each video sample, to obtain a visual-semantic representation of the video. There are different ways in which these could be combined. We choose to concatenate them, but first map them to a common space, which is helpful since at test time we will not have the semantic component.

Specifically, we map the semantic representation $a(y_i)$ to a space that matches the dimensionality of the visual features x_i . We use a multi-layer perceptron (MLP) for this, which consists of two fully connected (FC) layers and a ReLU. This MLP is trained with a least-square embedding loss to minimize the distance between x_i and the output from the MLP, which we call $a'(y)$. We use the visual feature space as the common embedding space [43].

Now we can concatenate x_i and $a'(y)$ to obtain a visual-semantic representation of each video. Using this representation, we compute k clusters using the k-means algorithm. Each cluster j has an initial cluster centroid or representative c_j , that is the average of all visual-semantic representations in that particular cluster.

3.3. Coarse-to-fine Network

We propose to use a coarse-to-fine network for ZSL, where each coarse representation of a video is obtained using the cluster centroids that the input video is closer to, and the fine representation is the final classification result of the input video. An overview of this network is seen in Figure 3.

Given input video feature x_i , the coarse part of the network outputs an intermediate representation z_i . Concatenating x_i and z_i we obtain the coarse representation ω_i .

We now use the clusters to pull the coarse representation closer to the nearest centroids, and thus clean outliers. For this, we compute the Euclidean distance to each cluster j , which we refer to as $d_{i,j}$, take its inverse (i.e $1/d_{i,j}$) and normalize the distances using their maximum and minimum values. We represent these normalized values using $\theta_{i,j}$, and will serve as the weights of each cluster centroid in the final coarse representation b_i :

$$b_i = \omega_i + \sum_{j=1}^k \theta_{i,j} c_j \quad (1)$$

This coarse representation b_i is the input to the fine network, which is simply an MLP. The output of the fine network is a vector corresponding to the total number of seen

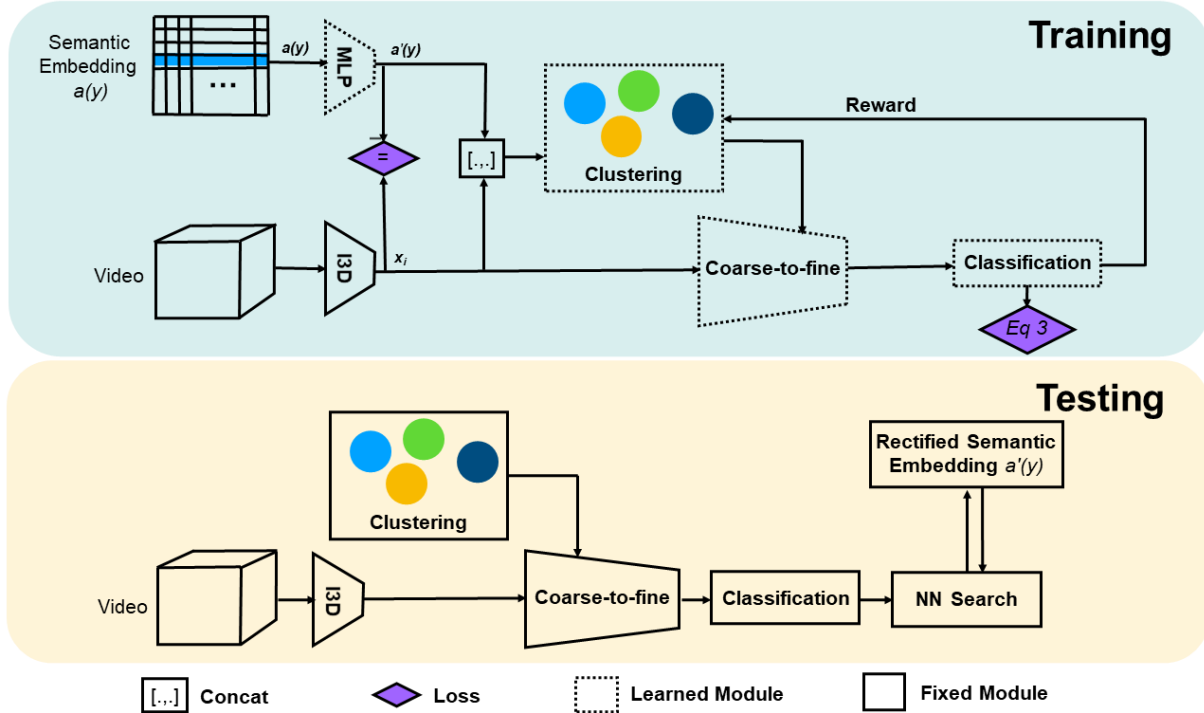


Figure 2. Overview of CLASTER. We train a MLP to obtain a joint visual-semantic embedding per instance. We cluster these with k-means to obtain initial cluster representatives. We compute a coarse representation of the video that helps in identifying the nearest clusters. We then obtain a weighted representation of all clusters and this is used as input to the fine network which performs the final classification. Based on the classification result, we send a reward and optimize the clusters using REINFORCE. At test time, we perform fully supervised classification on the seen classes and then do a nearest neighbor search with the rectified semantic embeddings to predict the unseen class.

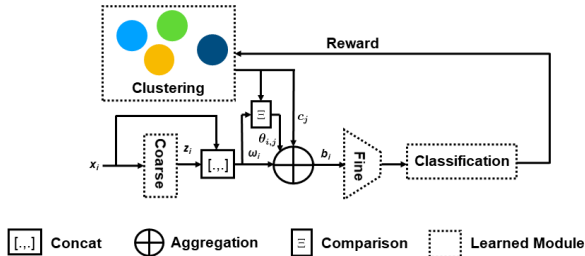


Figure 3. Overview of coarse-to-fine network. The input to the coarse network is an I3D feature vector and the output of the coarse network is concatenated with this input to obtain a coarse representation of the video that is then mapped to the clusters. An aggregated representation of the video with the clusters is obtained and this is used as input to the fine network, which then performs fine-grained classification.

classes, obtained by using a custom semantic softmax function described in the next subsection. The implementation details of the architecture of both networks is defined in Section 4.2.

3.4. Loss Function

We inject additional supervision right before classification, by using a semantic softmax function, inspired by Ji et al. [14], defined as:

$$\hat{y}_i = \frac{e^{a(y_i)^T V(b_i)}}{\sum_{j=1}^S e^{a(y_j)^T V(b_i)}}, \quad (2)$$

where S is the total number of seen classes, $V(b_i)$ is the feature representation in the layer before the softmax and the output \hat{y}_i is a vector with a probability distribution over the seen classes.

We use the natural choice to train a multi-class probabilistic classifier, which is the cross-entropy loss with a regularization term:

$$\min_W \sum_{i=1}^N \mathcal{L}(x_i) + \lambda \|W\|_F^2. \quad (3)$$

3.5. Optimization by Reinforcement Learning

Given the probabilistic prediction \hat{y}_i and the one-hot representation of the ground truth class y_i , we compute a classification score $sc = y_i \cdot \hat{y}_i$. Also, to obtain the reward we

check if argmax of \hat{y}_i and y_i lie in the same index. We save this as arg_i and set it to 1 if TRUE and 0 otherwise. Now we can update the cluster centroid c_j closest to ω_i using the REINFORCE [18] algorithm. We calculate the reward r based on the classification score obtained, as in:

$$r = \begin{cases} 1 & \text{if } \text{arg}_i = 1 \\ -1 & \text{if } \text{arg}_i = 0 \end{cases} \quad (4)$$

This essentially gives a positive reward if the model has predicted a correct classification and a negative reward if the classification was incorrect. This formulation is inspired by Likas [18], where it is used for competitive learning.

We compute Δc_j as the update of c_j as:

$$\Delta c_j = \alpha(r - \beta_j) \frac{\partial \ln g_j}{\partial c_j}, \quad (5)$$

where α is a fixed learning rate, r is the reward, β_j is called the reinforcement baseline, $\frac{\partial \ln g_j}{\partial c_j}$ is called the characteristic eligibility of cluster centroid c_j , which quantifies the match of a cluster j with respect to a given input, and is approximated as:

$$\frac{\partial \ln g_j}{\partial p_j} = \frac{sc - p_j}{p_j(1 - p_j)}, \quad (6)$$

and $p_j = 2(1 - f(\theta_{i,j}))$ and $f(x) = \frac{1}{1 + e^{-x}}$. Substituting Eq. 6 in Eq. 5, we obtain:

$$\Delta c_j = \alpha(r - \beta_j) \frac{\partial \ln g_j}{\partial p_j} \frac{\partial p_j}{\partial \theta_{i,j}} \frac{\partial \theta_{i,j}}{\partial c_j} \quad (7)$$

From Eq. 6 and the definition of p_j , we get to:

$$\Delta c_j = \alpha(r - \beta_j)(sc - p_j) \frac{\partial \theta_{i,j}}{\partial c_j}. \quad (8)$$

If we consider our distance metric as Euclidean and set β_j as zero, we obtain Eq. 9 as the updating rule for the cluster centroid c_j :

$$\Delta c_j = \alpha r (sc - p_j) (\omega_i - c_j) \quad (9)$$

For further details on this derivation, please refer to Likas [18]. The only difference is that we do not consider our clusters to be Bernoulli units, where the modification of the cluster representative is discrete (either 0 or 1). Instead, we modify the cluster with the range of values of sc , which is between 0 and 1.

3.6. Rectification of the Semantic Embedding

Sometimes, in ZSL, certain data points tend to appear as nearest-neighbor of many other points in the projection space. This is referred to as the hubness problem [34].

We avoid this problem using semantic representation rectification [20], where the class representation is modified by averaging the output generated by the projection

network, which in our case is the MLP of the fine network. Specifically, for the unseen classes, we perform rectification by first using the MLP trained on the seen classes to project the semantic embedding and then to that add the average of projected semantic embeddings from the k -nearest neighbors of the seen classes, as in:

$$\hat{a}(y_i) = a'(y_i) + \frac{1}{k} \sum_{n \in N} \cos(a'(y_i), n) \cdot n, \quad (10)$$

where, $a'(y)$ refers to the projection of y using the trained MLP, $\cos(a, n)$ refers to the cosine similarity between a and n , the operator \cdot refers to the dot product and N refers to the k -nearest neighbors of $a'(y_{u_i})$.

3.7. Nearest Neighbor Search

At test time in the ZSL, given a test video, we predict a seen class and compute or retrieve its semantic representation. After rectification, we find the nearest neighbor in the set of unseen classes.

In the GZSL task, class predictions may be of seen or unseen classes. Thus, we first use a bias detector [9] which helps us detect if the video belongs to the seen or unseen class. If it belongs to a seen class, we predict the class directly from our model. If the video belongs to an unseen class, we proceed as in ZSL.

3.8. Semantic embedding of action classes

Some datasets, such as HMDB51 [16], do not have semantic manual annotations. Instead, these semantic representations are often computed using a word2vec model pre-trained on Google news [24]. In most action recognition datasets, actions labels are phrases rather than single words (e.g. ‘‘playing guitar’’). In this scenario, the word2vec embeddings of each word are averaged to obtain the embedding for the entire phrase. This works in some cases, however, simple averaging does not always capture the interdependency of action classes. For example, pairs such as ‘‘jumping jacks’’ and ‘‘jumping ropes’’ or ‘‘horse riding’’ and ‘‘horse racing’’ lie far apart in the word2vec space, as the average of the words do not lie close to related words in the same space.

To alleviate this, we propose the use of sentence2vec [28], an embedding model which is designed to capture the meaning of sentences. Specifically, sentence2vec learns embeddings with respect to the sentence context, rather than a fixed window of context words (as in word2vec). It represents the sentence context as n -grams and optimizes the additive combination of the word vectors to obtain sentence embeddings. Sentence2vec is capable of producing good embeddings for the phrases that typically make up the labels of action classes. Figure 4 illustrates how the neighbors

change and become more meaningful when we move from `word2vec` to `sentence2vec`.

We show in sections 4.4 and 4.5 that using `sentence2vec` over `word2vec` significantly improves performance of some of the recent state-of-the-art approaches. It also helps reach performance close to using manual semantic representation. This suggests the potential of using `sentence2vec` on large scale datasets instead of having to manually annotate them.

4. Experimental Analysis

In this section, we look at the qualitative and quantitative performance of our model. We first describe the experiment settings, and then show a thorough ablation study, that explores the contribution of each component. We then compare the proposed method to the state-of-the-art in the ZSL and GZSL tasks, and give analytical insights into the advantages of CLASTER.

4.1. Datasets

We choose the Olympic Sports [26], HMDB-51 [16] and UCF-101 [36], so that we can compare to recent state-of-the-art in zero-shot action recognition [8, 22, 29]. They contain 783, 6766 and 13320 videos, and have 16, 51 and 101 classes, respectively. We follow the commonly used 50/50 splits proposed by Xu et al. [40], where 50 percent are seen classes and 50 are unseen classes. Similar to other approaches [44, 8, 29, 23, 15], we report average accuracy and standard deviation over 10 independent runs.

4.2. Implementation Details

Visual features. We use RGB and flow features extracted from the *Mixed 5c* layer of an I3D network pre-trained on the Kinetics [3] dataset. The *Mixed 5c* output of the flow network is averaged across the temporal dimension and pooled by four in the spatial dimension and then flattened to a vector of size 4096. We then concatenate the two to get video features of size 8192.

Network architecture. The coarse part of the network is a two-layer fully connected network, whose output after concatenation with the video feature has the same dimensions as the cluster representatives. The size of the FC layers are 8192 each. The fine part of the network consists of two convolutional layers and two fully connected layers, where the last layer equals the number of unseen classes in the dataset we are looking at. All the modules are trained with the Adam optimizer with a learning rate of 0.0001 and weight decay of 0.0005.

RL optimization. We use 10,000 iterations and the learning rate α is fixed to 0.1 for the first 1000 iterations, 0.01 for the next 1000 iterations and then drop it to 0.001 for the remaining iterations.

Semantic embeddings. We use three types of embeddings to obtain semantic representations of the classes. We have human annotated semantic representations for UCF101 and the Olympic sports dataset of sizes 40 and 115 respectively. HMDB51 does not have human annotated semantic representations. Instead, we use a skip-gram model trained on the news corpus provided by Google to generate `word2vec` embeddings. Using action classes as input, we obtain a vector representation of 300 dimensions. Some class labels contain multiple words. In those cases, we use the average of the `word2vec` embeddings. We also use `sentence2vec` embeddings, trained on Wikipedia. These can be obtained for both single words and multi-word expressions.

4.3. Ablation Study

We test using different number of clusters and show the results in Figure 5. These are for 5 runs on random splits. As we can see, the average accuracy increases until 6 clusters, and after that remains more or less constant. Thus, we use 6 clusters.

We show the performance of using the different components of CLASTER in Table 1. We consider no clustering, (which in our case is the equivalent of having a single cluster) random clustering and the standard k-means. We observe that using clusters is beneficial, but only if they are meaningful, as in the case of K-means.

We observe that using semantic embedding rectification improves the accuracy, as the chances of reaching previously unreachable classes increased to an extent. We also compare the standard softmax function and the semantic softmax function, which provides additional supervision at the time of obtaining the predicted probabilities, and results in a small increase in the accuracy. We finally show that the clustering optimization with RL causes a huge boost in the performance. Section 4.6 explores how the clusters change after this optimization. In a nutshell, the RL optimization essentially makes the clusters cleaner moving most instances in a class to the same cluster.

4.4. Results on ZSL

We compare our approach to several state-of-the-art methods: the out-of-distribution detector method (OD) [22], a generative approach to zero-shot action recognition (GGM) [25], the evaluation of output embeddings (SJE) [1], the feature generating networks (WGAN) [39] and prototype sampling graph neural network (PS-GNN) [10]. While recent approaches use a pre-trained model on Sports-1M dataset [25] or Kinetics [22, 39], we use a pre-trained model on Kinetics.

We observe that the proposed CLASTER consistently outperforms other state-of-the-art approaches. Results are shown in Table 2. On the HMDB51 dataset, it improves 4.0% over the next best performing model PS-GNN [10].

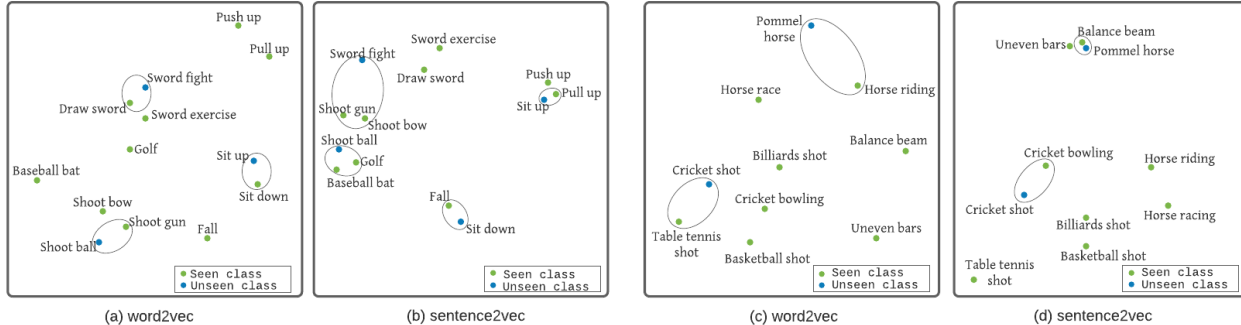


Figure 4. **HMD51** (a) Averaging word embeddings can produce poor results in certain cases. For example the nearest neighbor of “shoot ball” is “shoot gun”, and of “sit up” is “sit down” which are not necessarily meaningful (b) Sentence2vec better captures phrase meanings: Nearest neighbors to “sit up” is now “push up”, and for “shoot ball”, is golf. **UCF101** (c) The same effect is observed, where after averaging word2vec representations, the nearest neighbor of “pommel horse” is ”horse riding” (d) Sentence2vec helps capture phrase meanings: the while nearest neighbor of “pommel horse” is now “balance beam”. The circles contain the nearest neighbor to the given unseen class and is for illustration purposes.

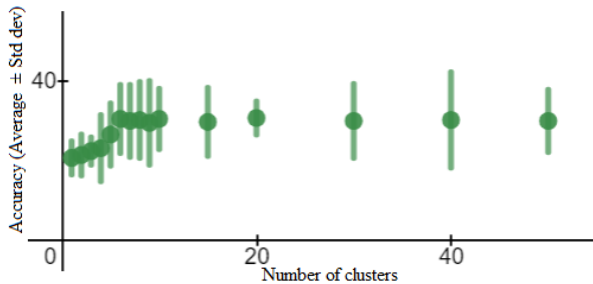


Figure 5. Effect of using different number of clusters. The green line represents the standard deviation. The reported accuracy is on the UCF101 dataset. As can be seen, the average cluster accuracy increases till about 6 clusters and then remains more or less constant. The vertical lines correspond to the standard deviation.

Component	UCF101 accuracy
No clustering	31.6 ± 4.6
Random clustering (K=6)	24.1 ± 6.3
K-means (K=6)	35.3 ± 3.9
K-means + R	37.1 ± 2.7
K-means + R + Semantic softmax	37.5 ± 3.2
CLUSTER: Full model with RL	46.4 ± 5.1

Table 1. Ablation study of different components of our model on ZSL with word2vec. The accuracies correspond to accuracy averaged over 5 independent test runs along with the standard deviation. We first show the effect of using a well defined clustering algorithm. Next, we show the effect of adding ‘R’ which stands for rectification of semantic embeddings and then replace the standard soft-max with our proposed semantic softmax. Finally, the last row represents our proposed model. All the reported accuracies are on the same five splits, note that Table 2 is with 10 splits.

On UCF101 it improves 3.5% over the next best performing model, when using semantic manual annotations, and 3.7% when using word2vec. On the Olympics dataset,

Method	SE	Olympics	HMD51	UCF101
OD [22]	M	65.9 ± 8.1	-	38.3 ± 3.0
GGM [25]	M	57.9 ± 14.1	-	24.5 ± 2.9
SJE [1]	M	47.5 ± 14.8	-	12.0 ± 1.2
WGAN [39]	M	64.7 ± 7.5	-	37.5 ± 3.1
CLUSTER (ours)	M	67.4 ± 7.8	-	41.8 ± 2.8
OD [22]	W	50.5 ± 6.9	30.2 ± 2.7	26.9 ± 2.8
PS-GNN [10]	W	61.8 ± 6.8	32.6 ± 2.9	43.0 ± 4.9
GGM [25]	W	41.3 ± 11.4	20.7 ± 3.1	20.3 ± 1.9
SJE [1]	W	28.6 ± 4.9	13.3 ± 2.4	9.9 ± 1.4
WGAN [39]	W	47.1 ± 6.4	29.1 ± 3.8	25.8 ± 3.2
CLUSTER (ours)	W	63.8 ± 5.7	36.6 ± 4.6	46.7 ± 5.4
OD*	S	50.8 ± 2.1	39.3 ± 3.1	35.9 ± 2.2
WGAN*	S	46.8 ± 4.2	34.7 ± 4.3	32.8 ± 5.4
CLUSTER (ours)	S	64.2 ± 3.3	41.8 ± 2.1	50.2 ± 3.8

Table 2. ZSL, comparison with prior work. The accuracies correspond to accuracy averaged over 10 independent test runs along with the standard deviation ‘SE’: semantic embedding, ‘M’: manual representation, W: word2vec embedding, S: sentence2vec. * run by us with author’s code.

CLUSTER improves 1.5% over the next best performing model OD [22] when using manual semantic representations; and 2% when using word2vec.

We measure the impact of using sentence2vec instead of word2vec. We test this on our own method, as well as as input to OD and WGAN, using the authors’ code. We show that sentence2vec significantly improves over using word2vec, especially on UCF101 and HMD51.

4.5. Results on GZSL

We now compare to the same approaches in the GZSL task in Table 3. Here CLUSTER outperforms all previous methods across different modalities. We obtain an improvement on average of 2.6% and 5% over the next best per-

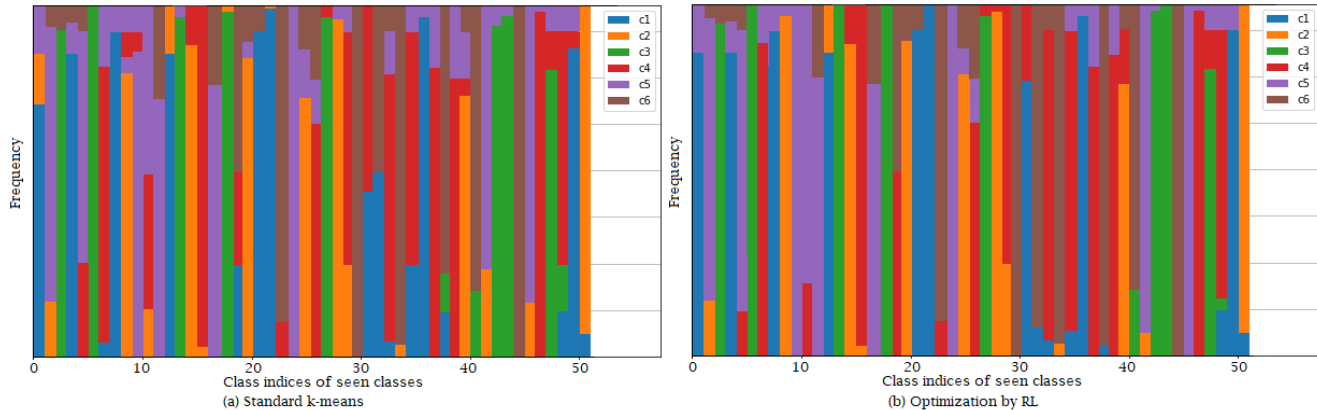


Figure 6. Analysis of how RL optimization changes the cluster to which an instance belongs. The frequencies are represented as percentages of instances in each cluster. We can see that the clusters are a lot "cleaner" after the optimization by RL.

Method	SE	Olympics	HMDB51	UCF101
OD [22]	M	66.2 ± 6.3	-	49.4 ± 2.4
GGM [25]	M	52.4 ± 12.2	-	23.7 ± 1.2
WGAN [39]	M	59.9 ± 5.3	-	44.4 ± 3.0
CLASTER (ours)	M	68.8 ± 6.6	-	50.9 ± 3.2
OD [22]	W	53.1 ± 3.6	36.1 ± 2.2	37.3 ± 2.1
PS-GNN [10]	W	52.9 ± 6.2	24.2 ± 3.3	35.1 ± 4.6
GGM [25]	W	42.2 ± 10.2	20.1 ± 2.1	17.5 ± 2.2
SJE [1]	W	32.5 ± 6.7	10.5 ± 2.4	8.9 ± 2.2
WGAN [39]	W	46.1 ± 3.7	32.7 ± 3.4	32.4 ± 3.3
CLASTER (ours)	W	58.1 ± 2.4	42.4 ± 3.6	42.1 ± 2.6
OD*	S	54.1 ± 2.7	42.3 ± 3.1	45.7 ± 2.3
WGAN*	S	47.6 ± 4.2	38.2 ± 4.1	40.2 ± 5.1
CLASTER (ours)	S	58.7 ± 3.1	47.4 ± 2.8	48.3 ± 3.1

Table 3. GZSL, comparison with prior work. The accuracies correspond to accuracy averaged over 10 independent test runs along with the standard deviation 'SE': semantic embedding, 'M': manual representation, W: word2vec embedding, S: sentence2vec. * run by us with author's code.

forming method on the Olympics dataset using manual representations and word2vec respectively. We obtain an average improvement of 6.3% over the next best performing model on the HMDB51 dataset using word2vec. We obtain an improvement on average performance by 1.5% and 4.8% over the next best performing model on the UCF101 dataset using manual representations and word2vec respectively. Similarly to ZSL, we show generalized performance improvements using sentence2vec.

4.6. Analysis of the RL optimization

How do the clusters change after the RL optimization? For each class in the training set, we measure the distribution of clusters that they belong to, visualized in Figure 6. Here, each column represents a class, and each color a cluster. In a perfect clustering, each row would have a single

color. We observe that after the RL optimization, the clustering becomes "cleaner". This is, most instances in a class belong to a dominant cluster. This effect can be measured using the purity of the cluster:

$$Purity = \frac{1}{N} \sum_{i=1}^k \max_j |c_i \cap t_j|, \quad (11)$$

where N is the number of data points (video instances in our case), k is the number of clusters, c_i is a cluster in the set of clusters, and t_j is the classification which has the maximum count for cluster c_i .

Poor clustering results in purity values close to 0, and a perfect clustering will return a purity of 1. Using k-means, the purity of the clusters is 0.77, while optimizing the clusters with RL results in a purity of 0.89.

Finally, we observe another interesting side effect of clustering. Some of the most commonly confused classes before clustering (e.g. ("Baby crawling" vs. "Mopping floor"), ("Breaststroke" vs. "front crawl"), ("Rowing vs. front crawl") actually are assigned to different clusters, and the confusion is largely resolved after clustering. This suggests that clusters are also used as a means to differentiate between similar classes.

5. Comparison over random splits for ZSL and GZSL

Since we are using random splits, it is important to consider the performance of our model against other state-of-the-art models OD [22] and WGAN [39] on the same splits for fair comparison. We show that on all datasets, we outperform both OD [22] and WGAN [39] for each of the 10 splits used. The comparison of this for both ZSL and GZSL can be seen in Figure 7. All the comparisons are done when using sentence2vec as the embedding.

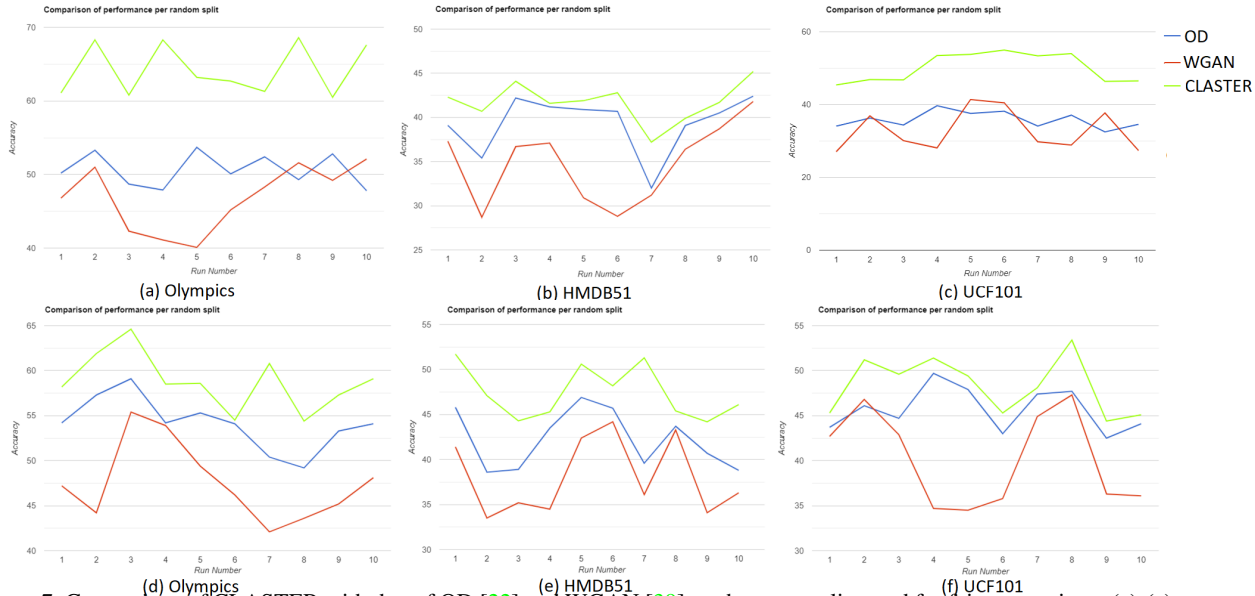


Figure 7. Comparison of CLUSTER with that of OD [22] and WGAN [39] on the same splits used for fair comparison. (a)-(c) corresponds to ZSL and (d)-(f) corresponds to GZSL. We can see that for every split used, we outperform both OD [22] and WGAN [39] in all comparisons.

6. Statistical Significance

We consider the dependent t-test for paired samples. This test is utilized in the case of dependent samples, in our case different model performances on the same random data split. This is a case of a paired difference test. This is calculated as shown in Eq 12.

$$t = \frac{\bar{X}_D - \mu_0}{s_D / \sqrt{n}} \quad (12)$$

Where \bar{X}_D is the average of the difference between all pairs and s_D is the standard deviation of the difference between all pairs. The constant μ_0 is zero in case we wish to test if the average of the difference is significantly different. Also, n represents the number of samples and $n - 1$ is the degrees of freedom used. The comparisons can be seen in Table 4. Lower the value of 'p', higher the significance.

As we can see, our results are statistically significant in comparison to both OD [22] and WGAN [39] in both ZSL and GZSL. However, in GZSL OD [22] also achieves results that are significant in comparison to WGAN [39].

7. Most Confused Classes

On different random splits, when occurring together as unseen classes the following classes appeared as most confused in UCF101: (Baby crawling, mopping floor),(band marching, military parade),(blow dry hair, haircut),(kayaking, rafting),(shaving beard, brushing teeth),(breaststroke, front crawl),(rowing, front crawl),(apply lipstick, apply eye makeup),(pommel horse

with other horse activities), (hammer throw and javelin throw). Using word2vec confuses pommel horse with other horse activities; groups all shooting activities together (basketball, table-tennis, billiards, cricket); walk (handstand walking and walking with a dog) hammer throw and javelin throw;

Similarly the most confused classes in HMDB51: (punch, draw sword),(fencing, shoot bow),(sword exercise, sword fight),(chew, smile),(drink, eat),(fencing, sword exercise) Using word2vec results in all sword related activities being confused; ride bike and ride horse (if both unseen then there is a confusion), all shooting related activities (ball, bow, gun); sit up and sit down;

Similarly the most confused classes in Olympics: (long jump, triple jump),(discus throw, hammer throw),(vault, high jump).

8. Conclusion

Zero-shot action recognition is the task of recognizing action classes without any visual examples. The challenge is to map the knowledge of seen classes at training time to that of novel unseen classes at test time. We propose a novel model that learns clustering-based representation optimized by reinforcement learning. Our method consistently outperforms prior work, regardless of the semantic embeddings used, the dataset, and, both, for standard and for generalized zero-shot evaluation (GZSL). Additionally, we show that better semantic representations of action classes can be obtained using sentence2vec instead of word2vec, as the former is specifically trained to capture the meaning of multi-

Pairs	Dataset	t-value	Statistical significance($p < 0.002$)	Type
CLUSTER and OD [22]	UCF101	-15.77	Significant, $p < 0.00001$	ZSL
CLUSTER and WGAN [39]	UCF101	-9.08	Significant, $p < 0.00001$	ZSL
OD [22] and WGAN [39]	UCF101	-1.70	Not Significant, $p = 0.12278$	ZSL
CLUSTER and OD [22]	HMDB51	-4.33	Significant, $p = 0.00189$	ZSL
CLUSTER and WGAN [39]	HMDB51	-5.54	Significant, $p = 0.00036$	ZSL
OD [22] and WGAN [39]	HMDB51	-3.71	Not Significant, $p = 0.00483$	ZSL
CLUSTER and OD [22]	Olympics	-9.06	Significant, $p < 0.00001$	ZSL
CLUSTER and WGAN [39]	Olympics	-11.73	Significant, $p < 0.00001$	ZSL
OD [22] and WGAN [39]	Olympics	-2.47	Not Significant, $p = 0.03547$	ZSL
CLUSTER and OD [22]	UCF101	-4.51	Significant, $p = 0.00148$	GZSL
CLUSTER and WGAN [39]	UCF101	-5.49	Significant, $p = 0.00039$	GZSL
OD [22] and WGAN [39]	UCF101	-3.16	Not Significant, $p = 0.01144$	GZSL
CLUSTER and OD [22]	HMDB51	-5.08	Significant, $p = 0.00066$	GZSL
CLUSTER and WGAN [39]	HMDB51	-7.51	Significant, $p = 0.00004$	GZSL
OD [22] and WGAN [39]	HMDB51	-5.27	Significant, $p = 0.00051$	GZSL
CLUSTER and OD [22]	Olympics	-5.79	Significant, $p = 0.00026$	GZSL
CLUSTER and WGAN [39]	Olympics	-8.39	Significant, $p = 0.00002$	GZSL
OD [22] and WGAN [39]	Olympics	-6.22	Significant, $p = 0.00014$	GZSL

Table 4. Comparison of the t-test for different pairs of models on the same random split. Lower the value of 'p', higher the significance. As we can see, our results are statistically significant in comparison to both OD [22] and WGAN [39] in both ZSL and GZSL. However, in GZSL OD [22] also achieves results that are significant in comparison to WGAN [39].

word expression such as the labels of action classes. Overall, we achieve remarkable improvements over the previously reported results, up to 11% absolute improvement on HMDB51 for GZSL.

References

- [1] Zeynep Akata, Scott Reed, Daniel Walter, Honglak Lee, and Bernt Schiele. Evaluation of output embeddings for fine-grained image classification. In *Proceedings of the IEEE conference on computer vision and pattern recognition*, pages 2927–2936, 2015. 2, 6, 7, 8
- [2] Humam Alwassel, Dhruv Mahajan, Lorenzo Torresani, Bernard Ghanem, and Du Tran. Self-supervised learning by cross-modal audio-video clustering. *arXiv preprint arXiv:1911.12667*, 2019. 2
- [3] J. Carreira and Andrew Zisserman. Quo vadis, action recognition? a new model and the kinetics dataset. In *IEEE Conf. Comput. Vis. Pattern Recog.*, 2017. 2, 3, 6
- [4] Yang Fan, Fei Tian, Tao Qin, Jiang Bian, and Tie-Yan Liu. Learning what data to learn. *arXiv preprint arXiv:1702.08635*, 2017. 3
- [5] Edward W Forgy. Cluster analysis of multivariate data: efficiency versus interpretability of classifications. *biometrics*, 21:768–769, 1965. 3
- [6] Chuang Gan, Ming Lin, Yi Yang, Gerard De Melo, and Alexander G Hauptmann. Concepts not alone: Exploring pairwise relationships for zero-shot video activity recognition. In *Thirtieth AAAI conference on artificial intelligence*, 2016. 3
- [7] Chuang Gan, Ming Lin, Yi Yang, Yueting Zhuang, and Alexander G Hauptmann. Exploring semantic inter-class relationships (sir) for zero-shot action recognition. In *Proceedings of the National Conference on Artificial Intelligence*, 2015. 3
- [8] Chuang Gan, Tianbao Yang, and Boqing Gong. Learning attributes equals multi-source domain generalization. In *Proceedings of the IEEE conference on computer vision and pattern recognition*, pages 87–97, 2016. 2, 6
- [9] Junyu Gao, Tianzhu Zhang, and Changsheng Xu. I know the relationships: Zero-shot action recognition via two-stream graph convolutional networks and knowledge graphs. In *Proceedings of the AAAI Conference on Artificial Intelligence*, volume 33, pages 8303–8311, 2019. 3, 5
- [10] Junyu Gao, Tianzhu Zhang, and Changsheng Xu. Learning to model relationships for zero-shot video classification. *IEEE Transactions on Pattern Analysis and Machine Intelligence*, 2020. 2, 3, 6, 7, 8
- [11] Rohit Girdhar and Deva Ramanan. Attentional pooling for action recognition. In *Advances in Neural Information Processing Systems*, pages 34–45, 2017. 2
- [12] Shreyank N Gowda, Panagiotis Eustratiadis, Timothy Hospedales, and Laura Sevilla-Lara. Alba: Reinforcement learning for video object segmentation. *arXiv preprint arXiv:2005.13039*, 2020. 3
- [13] Yanli Ji, Yue Zhan, Yang Yang, Xing Xu, Fumin Shen, and Heng Tao Shen. A context knowledge map guided coarse-to-fine action recognition. *IEEE Transactions on Image Processing*, 29:2742–2752, 2019. 2
- [14] Zhong Ji, Yuxin Sun, Yunlong Yu, Jichang Guo, and Yanwei Pang. Semantic softmax loss for zero-shot learning. *Neuro-*

- computing, 316:369–375, 2018. 4
- [15] Elyor Kodirov, Tao Xiang, Zhenyong Fu, and Shaogang Gong. Unsupervised domain adaptation for zero-shot learning. In *Proceedings of the IEEE international conference on computer vision*, pages 2452–2460, 2015. 6
- [16] Hildegard Kuehne, Hueihan Jhuang, Estíbaliz Garrote, Tomaso Poggio, and Thomas Serre. Hmdb: a large video database for human motion recognition. In *2011 International Conference on Computer Vision*, pages 2556–2563. IEEE, 2011. 5, 6
- [17] Christoph H Lampert, Hannes Nickisch, and Stefan Harmeling. Learning to detect unseen object classes by between-class attribute transfer. In *2009 IEEE Conference on Computer Vision and Pattern Recognition*, pages 951–958. IEEE, 2009. 2
- [18] Aristidis Likas. A reinforcement learning approach to online clustering. *Neural computation*, 11(8):1915–1932, 1999. 5
- [19] Bin Liu, Li Yao, Zheyuan Ding, Junyi Xu, and Junfeng Wu. Combining ontology and reinforcement learning for zero-shot classification. *Knowledge-Based Systems*, 144:42–50, 2018. 3
- [20] Changzhi Luo, Zhetao Li, Kaizhu Huang, Jiashi Feng, and Meng Wang. Zero-shot learning via attribute regression and class prototype rectification. *IEEE Transactions on Image Processing*, 27(2):637–648, 2017. 5
- [21] Laurens van der Maaten and Geoffrey Hinton. Visualizing data using t-sne. *Journal of machine learning research*, 9(Nov):2579–2605, 2008. 1
- [22] Devraj Mandal, Sanath Narayan, Sai Kumar Dwivedi, Vikram Gupta, Shuaib Ahmed, Fahad Shahbaz Khan, and Ling Shao. Out-of-distribution detection for generalized zero-shot action recognition. In *Proceedings of the IEEE Conference on Computer Vision and Pattern Recognition*, pages 9985–9993, 2019. 2, 3, 6, 7, 8, 9, 10
- [23] Pascal Mettes and Cees GM Snoek. Spatial-aware object embeddings for zero-shot localization and classification of actions. In *Proceedings of the IEEE International Conference on Computer Vision*, pages 4443–4452, 2017. 6
- [24] Tomas Mikolov, Ilya Sutskever, Kai Chen, Greg S Corrado, and Jeff Dean. Distributed representations of words and phrases and their compositionality. In *Advances in neural information processing systems*, pages 3111–3119, 2013. 2, 5
- [25] Ashish Mishra, Vinay Kumar Verma, M Shiva Krishna Reddy, S Arulkumar, Piyush Rai, and Anurag Mittal. A generative approach to zero-shot and few-shot action recognition. In *2018 IEEE Winter Conference on Applications of Computer Vision (WACV)*, pages 372–380. IEEE, 2018. 2, 6, 7, 8
- [26] Juan Carlos Niebles, Chih-Wei Chen, and Li Fei-Fei. Modeling temporal structure of decomposable motion segments for activity classification. In *European conference on computer vision*, pages 392–405. Springer, 2010. 6
- [27] Junhyuk Oh, Satinder Singh, Honglak Lee, and Pushmeet Kohli. Zero-shot task generalization with multi-task deep reinforcement learning. In *International Conference on Machine Learning*, pages 2661–2670, 2017. 3
- [28] Matteo Pagliardini, Prakhar Gupta, and Martin Jaggi. Unsupervised learning of sentence embeddings using compositional n-gram features. In *Proceedings of NAACL-HLT*, pages 528–540, 2018. 2, 5
- [29] Jie Qin, Li Liu, Ling Shao, Fumin Shen, Bingbing Ni, Jiaxin Chen, and Yunhong Wang. Zero-shot action recognition with error-correcting output codes. In *Proceedings of the IEEE Conference on Computer Vision and Pattern Recognition*, pages 2833–2842, 2017. 3, 6
- [30] Zhaofan Qiu, Ting Yao, and Tao Mei. Learning spatio-temporal representation with pseudo-3d residual networks. In *proceedings of the IEEE International Conference on Computer Vision*, pages 5533–5541, 2017. 2
- [31] Marcus Rohrbach, Michaela Regneri, Mykhaylo Andriluka, Sikandar Amin, Manfred Pinkal, and Bernt Schiele. Script data for attribute-based recognition of composite activities. In *Eur. Conf. Comput. Vis.*, 2012. 2
- [32] Marcus Rohrbach, Michael Stark, György Szarvas, Iryna Gurevych, and Bernt Schiele. What helps Where - and Why? Semantic Relatedness for Knowledge Transfer. In *IEEE Conf. Comput. Vis. Pattern Recog.*, 2010. 2
- [33] Bernardino Romera-Paredes and Philip Torr. An embarrassingly simple approach to zero-shot learning. In *International Conference on Machine Learning*, pages 2152–2161, 2015. 2
- [34] Yutaro Shigeto, Ikumi Suzuki, Kazuo Hara, Masashi Shimbo, and Yuji Matsumoto. Ridge regression, hubness, and zero-shot learning. In *Joint European Conference on Machine Learning and Knowledge Discovery in Databases*, pages 135–151. Springer, 2015. 5
- [35] Karen Simonyan and Andrew Zisserman. Two-stream convolutional networks for action recognition in videos. In *Advances in neural information processing systems*, pages 568–576, 2014. 2
- [36] Khurram Soomro, Amir Roshan Zamir, and Mubarak Shah. Ucf101: A dataset of 101 human actions classes from videos in the wild. *arXiv preprint arXiv:1212.0402*, 2012. 6
- [37] Du Tran, Lubomir Bourdev, Rob Fergus, Lorenzo Torresani, and Manohar Paluri. Learning spatiotemporal features with 3d convolutional networks. In *Proceedings of the IEEE international conference on computer vision*, pages 4489–4497, 2015. 2
- [38] Xiaolong Wang, Ross Girshick, Abhinav Gupta, and Kaiming He. Non-local neural networks. In *Proceedings of the IEEE conference on computer vision and pattern recognition*, pages 7794–7803, 2018. 2
- [39] Yongqin Xian, Tobias Lorenz, Bernt Schiele, and Zeynep Akata. Feature generating networks for zero-shot learning. In *Proceedings of the IEEE conference on computer vision and pattern recognition*, pages 5542–5551, 2018. 6, 7, 8, 9, 10
- [40] Xun Xu, Timothy Hospedales, and Shaogang Gong. Transductive zero-shot action recognition by word-vector embedding. *International Journal of Computer Vision*, 123(3):309–333, 2017. 2, 6
- [41] Xun Xu, Timothy M Hospedales, and Shaogang Gong. Multi-task zero-shot action recognition with prioritised data

- augmentation. In *European Conference on Computer Vision*, pages 343–359. Springer, 2016. 2
- [42] Zhiquan Ye, Yuxia Geng, Jiaoyan Chen, Jingmin Chen, Xiaoxiao Xu, SuHang Zheng, Feng Wang, Jun Zhang, and Huajun Chen. Zero-shot text classification via reinforced self-training. In *Proceedings of the 58th Annual Meeting of the Association for Computational Linguistics*, pages 3014–3024, 2020. 3
- [43] Li Zhang, Tao Xiang, and Shaogang Gong. Learning a deep embedding model for zero-shot learning. In *Proceedings of the IEEE Conference on Computer Vision and Pattern Recognition*, pages 2021–2030, 2017. 3
- [44] Yi Zhu, Yang Long, Yu Guan, Shawn Newsam, and Ling Shao. Towards universal representation for unseen action recognition. In *Proceedings of the IEEE Conference on Computer Vision and Pattern Recognition*, pages 9436–9445, 2018. 2, 6